

Chapter 6

Two-Dimensional Correlation Spectroscopy



Mirosław A. Czarnecki and Shigeaki Morita

Abstract Two-dimensional (2D) correlation spectroscopy is a well-established method for analysis of perturbation-induced spectral changes in various kinds of data. Due to selective correlation of the peaks and resolution enhancement, it provides useful information on the dynamics of spectral changes and enables more reliable band assignments. The generalized 2D correlation approach permits to apply various kinds of perturbations and makes possible for correlation between data obtained from different experiments (hetero-correlation). At the beginning of this chapter are shown the basic principles of 2D correlation spectroscopy together with the rules for interpretation of the synchronous and asynchronous spectra. Next, we report new developments in this method like sample–sample correlation spectroscopy and perturbation–correlation moving-window 2D correlation spectroscopy. Finally, are shown selected examples of successful applications of 2D correlation spectroscopy for study of interactions and molecular structure.

Keywords 2D correlation spectroscopy · Sample–sample correlation spectroscopy · Perturbation–correlation moving-window 2D correlation spectroscopy · Applications of 2D correlation NIR spectroscopy

6.1 Introduction

Two-dimensional (2D) correlation spectroscopy was introduced to vibrational spectroscopy by Isao Noda in 1986 [1]. In its original form, this method was dedicated to small-amplitude periodic perturbations, and hence, the area of its applications was limited—mainly to polymer studies [2, 3]. A breakthrough has started in 1993 after development of the generalized two-dimensional correlation spectroscopy (2DCOS)

M. A. Czarnecki (✉)

Faculty of Chemistry, University of Wrocław, F. Joliot-Curie 14, 50-383 Wrocław, Poland
e-mail: miroslaw.czarnecki@chem.uni.wroc.pl

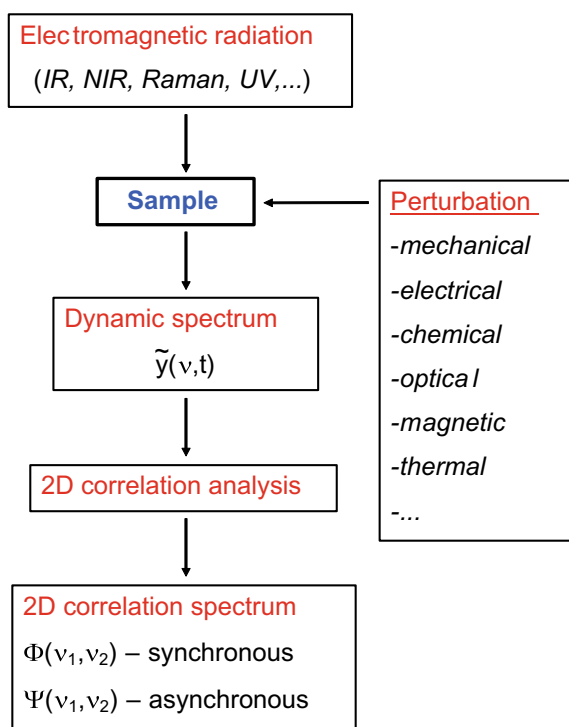
S. Morita

Faculty of Engineering, Osaka Electro-Communication University, Neyagawa, Japan
e-mail: smorita@isc.osakac.ac.jp

[4]. This new approach allows to accept any kind of perturbations and permits the hetero-correlations between the data obtained from different methods, such as MIR-NIR, MIR-Raman, UV-MIR and so on. In this way, the generalized 2D correlation analysis has begun a powerful and versatile tool for analysis of spectral data from various experiments [5]. This approach appears to be particularly useful in near-infrared (NIR) region since NIR spectra are very complex due to overlap of numerous overtones and combination bands [6, 7]. In addition, 2DCOS spectroscopy solves the problem of multicollinearity by independent correlation of variables.

The idea behind 2DCOS is very simple and is displayed in Fig. 6.1. The sample is subjected to external perturbation, which generates the specific changes at a molecular level. These changes can be monitored by any kind of electromagnetic radiation, including NIR. As a result, the measurements provide a series of perturbation-dependent spectra. From the single spectra $y(\nu, t)$, a perturbation-ordered data matrix is assembled:

Fig. 6.1 General scheme of 2D correlation spectroscopy



$$\begin{bmatrix} y(\nu_1, t_1) & y(\nu_2, t_1) & \cdots & y(\nu_m, t_1) \\ y(\nu_1, t_2) & y(\nu_2, t_2) & \cdots & y(\nu_m, t_2) \\ y(\nu_1, t_3) & y(\nu_2, t_3) & \cdots & y(\nu_m, t_3) \\ \cdots & \cdots & \cdots & \cdots \\ y(\nu_1, t_n) & y(\nu_2, t_n) & \cdots & y(\nu_m, t_n) \end{bmatrix} \quad (6.1)$$

where ν means wavenumber (or the other units), t is the value of perturbation, n is the number of spectra and m is the number of data points in the spectrum. Usually, this matrix is row-oriented; in the other case, one has to transpose the data. Prior to 2D correlation analysis, the perturbation-ordered data matrix is converted into the dynamic spectrum (\tilde{y}) by subtraction of the reference spectrum (\hat{y}):

$$\tilde{y}(\nu, t) = \begin{cases} y(\nu, t) - \hat{y}(\nu) & \text{for } t_{\min} \leq t \leq t_{\max} \\ 0 & \text{otherwise} \end{cases} \quad (6.2)$$

In principle, one can select an arbitrary reference spectrum, but usually, a perturbation-average spectrum is used as a reference:

$$\hat{y}(\nu) = \frac{1}{n} \cdot \sum_{i=1}^n y(\nu, t_i) \quad (6.3)$$

The proper selection of reference spectrum appreciably simplifies synchronous and asynchronous contour plots, since the peaks are developed only at the positions where intensity changes occur. This means that if the applied perturbation does not induce the spectral changes at given position, this peak does not appear in the correlation spectrum. 2D correlation analysis yields synchronous (Φ) and asynchronous (Ψ) spectra, which are a product of two or three matrices:

$$\Phi(\nu_i, \nu_j) = \frac{1}{n-1} \tilde{y}(\nu_i, t)^T \cdot \tilde{y}(\nu_j, t) \quad (6.4)$$

$$\Psi(\nu_i, \nu_j) = \frac{1}{n-1} \tilde{y}(\nu_i, t)^T \cdot M \cdot \tilde{y}(\nu_j, t) \quad (6.5)$$

where M is Hilbert–Noda transformation matrix [8]:

$$M_{i,j} = \begin{cases} 0 & \text{if } i = j \\ \frac{1}{\pi \cdot (j-i)} & \text{otherwise} \end{cases} \quad (6.6)$$

The specific information obtained from 2DCOS primarily depends on the sample properties, kind of external perturbation and the electromagnetic probe. The perturbation should stimulate the sample and generate specific variations of physicochemical properties at a molecular level. These variations may result from changes of time,

sample composition, temperature, pressure, pH and so on. Each kind of perturbation yields unique information about studied system. It is also important to apply an appropriate probe to successfully monitor the perturbation-induced changes in the studied system.

As mentioned before, the generalized 2DCOS permits for hetero-correlation of two unlike types of data; however, both data sets have to be recorded under the same perturbation values. If \tilde{y} and \tilde{u} are the dynamic spectra from two different experiments, then the synchronous and asynchronous hetero-correlation spectra are expressed:

$$\Phi(\nu_i, \mu_j) = \frac{1}{n-1} \tilde{y}(\nu_i, t)^T \cdot \tilde{u}(\mu_j, t) \quad (6.7)$$

$$\Psi(\nu_i, \mu_j) = \frac{1}{n-1} \tilde{y}(\nu_i, t)^T \cdot M \cdot \tilde{u}(\mu_j, t) \quad (6.8)$$

The properties of the synchronous and asynchronous spectra were explained by using the simulated spectra (Fig. 6.2). A data series consist of 11 spectra and each spectrum includes five peaks. The arrows point the direction of intensity changes. Figure 6.3 shows the corresponding synchronous and asynchronous spectra. As can be seen, the synchronous spectrum includes both the diagonal and cross-peaks. The diagonal peaks are always positive and represent the overall extent of intensity changes at individual wavenumbers. The cross-peaks are positive or negative and yield information on similarities of spectral changes at two different wavenumbers (ν_1, ν_2). The synchronous cross-peaks are positive if the spectral changes at ν_1 and ν_2 are in the same direction (both increasing or both decreasing) (Fig. 6.3a). The negative sign means the opposite. Such positive synchronous cross-correlation suggests that the changes at ν_1 and ν_2 originate from the same molecular fragment or two different fragments strongly interacting. In contrast, the asynchronous spectrum includes only the cross-peaks and yields information on differences of spectral

Fig. 6.2 A series of 11 simulated spectra. Each spectrum includes five peaks approximated by a product of Gauss and Lorentz function. The initial intensities were 1 and the final were 1.2 (5000 cm^{-1}), 0.8 (5500 cm^{-1}), 1 (6000 cm^{-1}), 1.1 (6500 cm^{-1}) and 0.9 (7000 cm^{-1}). The arrows show direction of the changes

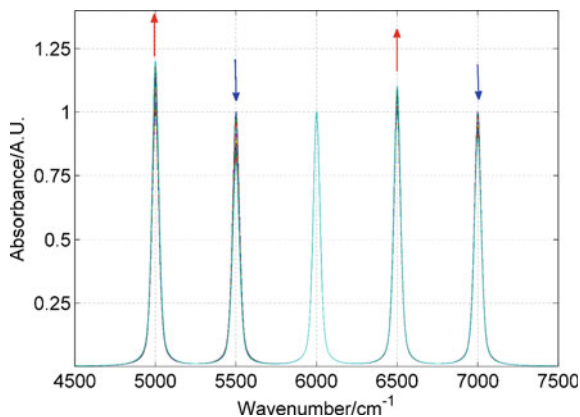
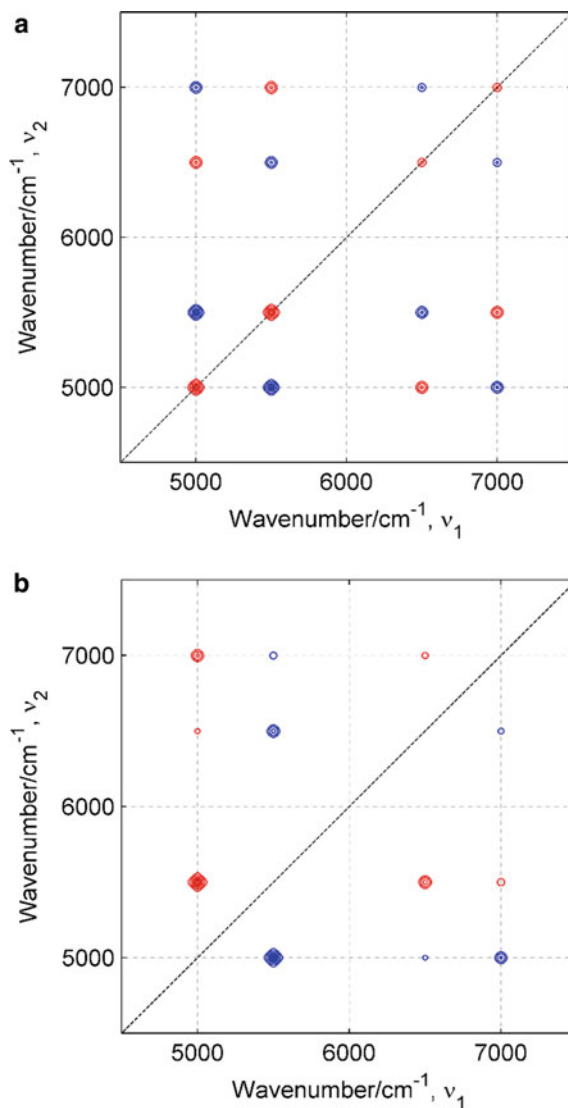


Fig. 6.3 Synchronous and asynchronous spectra obtained from the spectra shown in Fig. 6.2



changes at ν_1 and ν_2 (Fig. 6.3b). The presence of the asynchronous peak at (ν_1, ν_2) evidences that the spectral changes at ν_1 and ν_2 occur at different rate or are shifted in-phase. This way, one can differentiate the spectral responses from various components of the sample. This is an important feature of 2DCOS, which allows for the resolution enhancement. Irrespective of the separation, the peaks are resolved in the asynchronous spectrum as long as their spectral responses follow different pattern. To easy interpretation of 2D asynchronous contour plots, one can multiply the asynchronous intensity at (ν_1, ν_2) by the sign of the synchronous intensity at the same

coordinate. Hence, the presence of the positive asynchronous peak at (ν_1, ν_2) means that the spectral changes at ν_1 occur earlier/faster than those at ν_2 . The negative sign of the asynchronous peak means the opposite behavior. Selective correlation of the peaks in 2DCOS spectra allows for establishing of the origin of the peaks and easy the band assignment. Particularly useful are hetero-correlation spectra, which show the selective correlation between known and unknown spectral features.

The rules for interpretation of 2DCOS spectra are straightforward [4, 5]; however, correct interpretation of the real-world data is not always easy. Firstly, an application of the external perturbation is often accompanied by side effects. To obtain a ‘net’ information on the effect of interest, at first, one has to remove these side effects. The procedure, which removes these side effects depends on their specific nature, but in many cases, the normalization of the spectra significantly improves the quality of 2D contour plots [9]. Secondly, 2DCOS spectra, particularly the asynchronous ones, are very sensitive to noise, baseline fluctuation and other distortions. Besides, interpretation of 2DCOS spectra is complicated by band position and/or width variations. All these effects may generate artifacts in the synchronous and asynchronous spectra. Therefore, the systematic studies were undertaken to recognize and eliminate (where possible) these effects from 2D correlation spectra [10–13].

Sometimes, the spectral changes of interest are obscured by the noise, baseline fluctuation or the other effects. The proper pretreatment of the experimental spectra may significantly improve the quantity and quantity of the information obtained from 2DCOS [7, 9, 10]. An extensive baseline fluctuation generates long streaks observed in the synchronous and asynchronous contour plots. In many cases, a simple offset of the spectra at selected reference point can significantly reduce this effect [7]. Sometimes are necessary more advanced corrections by using polynomial functions. In an extreme case, one can use the second derivative spectra, instead of the original data, for the analysis [12]. The high level of noise will produce a lot of artifacts, especially in the asynchronous spectrum. The most popular methods of smoothing are based on Savitzky–Golay algorithm. The more advanced methods employ Fourier or wavelet filtering, or principal component analysis (PCA). Also, normalization of the spectra is often used as a pretreatment method. This way, one can eliminate the effects of varying concentration, temperature, pressure or sample thickness on the 2DCOS spectra [9].

2D correlation spectroscopy offers a significant simplification of the complex NIR spectra. However, the most important advantage of using 2DCOS in NIR region is the ability of resolving of highly overlapped peaks. Besides, selective correlation between MIR (or Raman) and NIR spectra allows for reliable band assignment in NIR region and obtain information on the molecular structure and interactions [6, 7].

6.2 New Developments in Two-Dimensional Correlation Spectroscopy

6.2.1 Sample–Sample Correlation Spectroscopy

For the last two decades or so, several new ideas regarding 2DCOS have been proposed such as sample–sample (SS), moving-window two-dimensional (MW2D) and perturbation-correlation moving-window two-dimensional (PCMW2D). Here, SS, MW2D and PCMW2D methods will be outlined. The first idea of sample–sample correlation, i.e., opposite to conventional variable–variable correlation, was proposed by Zimba [14], and this idea was subsequently refined by Šašić et al. [15, 16]. As given in Eq. (4), the conventional synchronous 2D correlation spectrum $\Phi(v_i, v_j)$ is calculated as a covariance matrix of $y(v, t)$. The synchronous sample–sample correlation (Φ_{SS}) is given as a covariance matrix of transposed $y(v, t)$ matrix, and the asynchronous sample–sample correlation (Ψ_{SS}) is calculated as:

$$\Phi_{SS}(t_k, t_l) = \frac{1}{m-1} \tilde{y}(v, t_k) \cdot \tilde{y}(v, t_l)^T \quad (6.9)$$

$$\Psi_{SS}(t_k, t_l) = \frac{1}{m-1} \tilde{y}(v, t_k) \cdot M \cdot \tilde{y}(v, t_l)^T \quad (6.10)$$

Figure 6.4 shows temperature-dependent diffuse reflectance NIR spectra of microcrystalline cellulose (MCC) and their second derivative spectra [17]. Figure 6.5 represents synchronous sample–sample 2D correlation spectrum constructed from the second derivative spectra shown in Fig. 6.4b. In the case of conventional 2D correlation spectra (not shown), correlation maps are spread between two spectral variable

Fig. 6.4 Temperature-dependent diffuse reflectance NIR spectra of microcrystalline cellulose (MCC) (a) and their second derivative spectra (b)

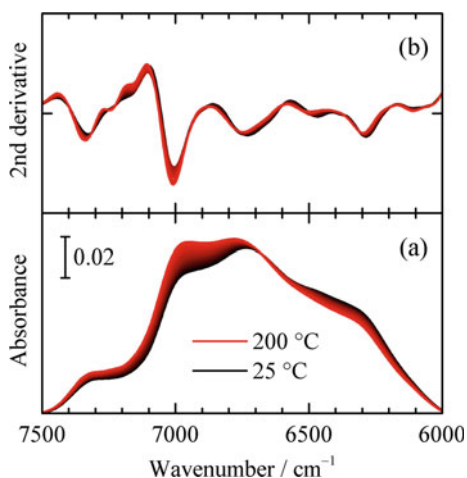
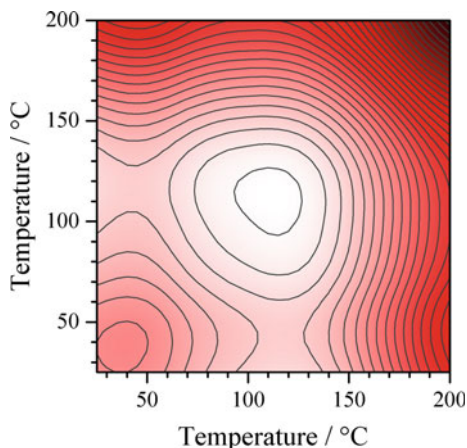


Fig. 6.5 Synchronous sample–sample 2D correlation map constructed from the second derivative spectra shown in Fig. 6.4



axes, e.g., wavenumber–wavenumber axes. In contrast, in the case of sample–sample correlation, 2D correlation maps are spread between two sample variable axes, e.g., temperature–temperature axes, as shown in Fig. 6.5. Therefore, some informative sample points are visually identified in the 2D correlation maps by this method.

6.2.2 *Perturbation-Correlation Moving-Window Two-Dimensional (PCMW2D) Correlation Spectroscopy*

Thomas and Richardson proposed the first idea of MW2D correlation spectroscopy [18]. For a set of obtained spectra $y(\nu, t)$, j th window of submatrix consisting of $2w + 1$ spectra $y_j(\nu, t_j)$ is considered, where j and J are the index of window and that of a spectrum within the window, respectively. The MW2D correlation spectrum is obtained by incrementally sliding the window position along the perturbation variable direction from $j = 1 + w$ to $n - w$, where n is the number of spectra in $y(\nu, t)$, and calculating

$$\Omega_{A,j}(\nu, t_j) = \frac{1}{2w} \sum_{J=j-w}^{j+w} \tilde{y}_j^2(\nu, t_j) \quad (6.11)$$

This is an auto-correlation spectrum or variance spectrum calculated using the $2w + 1$ spectra in the window. Morita et al. [19] reported that the MW2D correlation intensities are proportional to a squared perturbation derivative, i.e.,

$$\Omega_A(\nu, t) \sim \left[\frac{\partial y(\nu, t)}{\partial t} \right]^2 \quad (6.12)$$

Another type of moving-window technique, PCMW2D correlation spectroscopy, was proposed by Morita et al. [20] In this case, both synchronous and asynchronous correlation spectra were calculated as

$$\Pi_{\Phi,j} = \frac{1}{2w} \sum_{J=j-w}^{j+w} \tilde{y}(\nu, t_J) \cdot \tilde{t}_J \quad (6.13)$$

$$\Pi_{\Psi,j} = \frac{1}{2w} \sum_{J=j-w}^{j+w} \tilde{y}(\nu, t_J) \cdot \sum_{K=j-w}^{j+w} M_{JK} \cdot \tilde{t}_K \quad (6.14)$$

where \tilde{t} and M are dynamic perturbation and Hilbert–Noda transformation matrix, respectively. As similar to MW2D correlation spectroscopy, following relations were found by Morita et al.

$$\Pi_{\Phi}(\nu, t) \sim \left[\frac{\partial y(\nu, t)}{\partial t} \right]_{\nu} \quad (6.15)$$

$$\Pi_{\Psi}(\nu, t) \sim - \left[\frac{\partial^2 y(\nu, t)}{\partial t^2} \right]_{\nu} \quad (6.16)$$

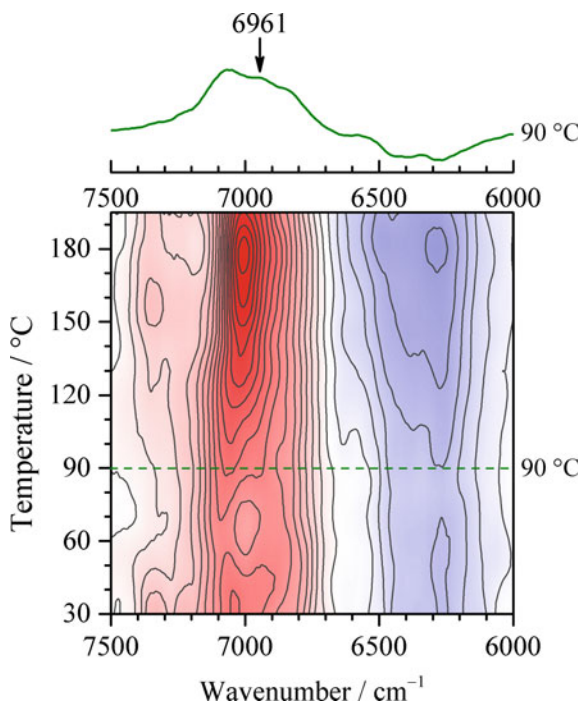
i.e., synchronous and asynchronous PCMW2D correlation intensities are proportional to a perturbation derivative and the opposite sign of a perturbation second derivative [20]. In the case of linear perturbation, therefore, synchronous and asynchronous PCMW2D correlation intensities are proportional to a gradient and a curvature of the spectral intensity variations along the perturbation direction, respectively [20].

Figure 6.6 shows synchronous PCMW2D correlation map constructed from the temperature-dependent NIR spectra of MCC shown in Fig. 6.4a. Positive and negative correlation intensities in the map represent increase and decrease of the spectral intensities along the temperature direction, respectively. A slice spectrum at 90 °C is also plotted in the figure. A positive correlation peak located at 6961 cm⁻¹ is reported to be intermediate hydrogen bonds in MCC [17].

6.3 Applications of Two-Dimensional Correlation NIR Spectroscopy

The simplicity in obtaining of 2D correlation spectra resulted in a fast development of this approach. In a short time, a number of successful applications of 2DCOS to various fields of chemistry were reported. In 1996, Noda et al. published the first application of 2DCOS in NIR region (2DCOS-NIR) to study self-association of oleyl alcohol in the liquid phase [21]. Due to the resolution enhancement, a number

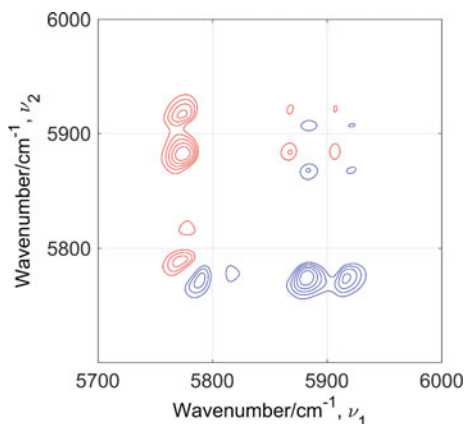
Fig. 6.6 Synchronous PCMW2D correlation map constructed from the temperature-dependent NIR spectra shown in Fig. 6.4. Positive and negative correlation intensities are colored by red and blue, respectively



of new peaks, not seen in the raw spectra, were resolved. The selective correlation of the peaks allowed proposing the molecular mechanism of the temperature-induced changes in hydrogen bonding for neat oleyl alcohol. Introduction of 2DCOS approach to NIR region inspired a number of interesting studies on various kinds of samples. The first applications were devoted to studies of hydrogen bonding in pure liquids like alcohols, water, NMA or fatty acids. A next important step was an application of 2DCOS-NIR to more complex systems including water solutions of proteins. These studies were focused mainly on examination of the secondary structure of proteins as a function of temperature, concentration or pH. An important area of employing of 2DCOS-NIR is polymer studies, with particular attention paid on the exploration of the structural response of the hydrogen bonds and hydrocarbon chains during heating, as well as stress-induced molecular chain deformation. Numerous works have been devoted to 2DCOS-NIR examination of the structure and interactions in binary mixtures of aqueous solutions of organic solvents like alcohols, NMA diols, aminoalcohols and diamines. Most of these studies have been recently reviewed [5–7]; hence, we focus our attention on new works.

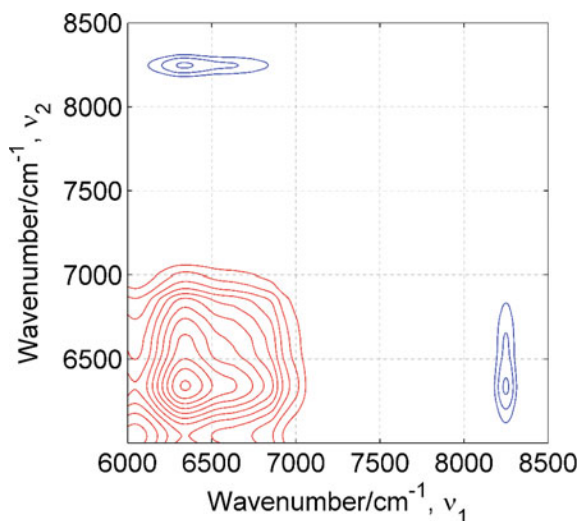
Kwaśniewicz and Czarnecki explored the spectra–structure correlations in MIR and NIR regions [22, 23]. The authors applied 2DCOS and chemometric methods for analysis of ATR-IR, Raman and NIR spectra of eight n-alkanes and seven 1-chloroalkanes in the liquid phase [22]. In both cases, the chain length variation was used as a perturbation. As can be seen (Fig. 6.7), the overtones of the CH stretching

Fig. 6.7 Asynchronous 2D correlation spectrum constructed from NIR spectra of n-alkanes. In red and blue are drawn the positive and negative peaks, respectively. (Reprinted from Ref. [22] with permission from Elsevier)



bands (near 5800 and 5900 cm⁻¹) show characteristic pairs of the peaks close to the diagonal. Owing to resolution enhancement in the asynchronous spectrum, for the first time, the contributions from the terminal and midchain methylene groups were observed in the spectra of liquid n-alkanes and 1-chloroalkanes. The same authors examined the effect of chain length on MIR and NIR spectra of aliphatic 1-alcohols from methanol to 1-decanol [23]. A negative correlation between the first overtone of the hydrogen-bonded OH (near 6300 cm⁻¹) and the second overtone of the methylene group (near 8225 cm⁻¹) (Fig. 6.8) reveals that the intensity changes for these two groups are in the opposite direction. Hence, an application of 2DCOS approach provides direct evidence that the degree of self-association of liquid 1-alcohols decreases with the chain length increase. It is worth to mention that the

Fig. 6.8 Synchronous 2DCOS-NIR spectra of 1-alcohols from 1-butanol to 1-decanol. In red and blue are drawn the positive and negative peaks, respectively



asynchronous contour plots made possible to identify the peaks from the terminal CH_2 next to OH and the peaks from the midchain CH_2 .

A lot of efforts were undertaken for examination of microheterogeneity in binary mixtures [24–27]. 2DCOS-NIR studies on propyl alcohols/water mixtures reveal the separation at a molecular level and the presence of homoclusters of water and alcohol existing in equilibrium with the mixed clusters (heteroclusters) [24]. The presence of these clusters is responsible for macroscopic structure of the mixtures and leads to anomalous physicochemical properties. In the water-poor region, the molecules of alcohols are in the same environment as those in the pure liquid alcohols, while the molecules of water are dispersed in the organic phase. When the water content increases, the molecules of water form clusters interacting with the OH groups of the alcohols. These results clearly show that the degree of microheterogeneity in alcohol/water mixtures is closely related to the extent of self-association of the alcohol.

Interestingly, similar conclusion was obtained from 2DCOS-NIR and chemometric studies of binary mixtures of methanol with short-chain aliphatic alcohols [25]. The degree of deviation from the ideal mixture is correlated with the chain length and the order of the alcohol. For most of the mixtures, the largest deviation from the ideality appears at equimolar mixture. The heteroclusters were observed in the whole range of mole fractions, while the homoclusters occur above a certain concentration limit. It is interestingly to note that the homoclusters of both components are similar as those observed in neat liquids.

In spite of similar structure and properties of methanol and its deuterated derivative, $\text{CH}_3\text{OH}/\text{CD}_3\text{OH}$ mixture also deviates from the ideal mixture [26]. The extent of this deviation is much smaller as compared with the mixtures of unlike alcohols [25], and it results mainly from the difference between the CH_3 and CD_3 groups. It is of note that the contribution to heterogeneity from the OH groups is relatively small. The $\text{CH}_3\text{OH}/\text{CD}_3\text{OH}$ mixture is composed of the homoclusters of both alcohols and the mixed clusters. The homoclusters in the mixture are similar to those present in neat alcohols. The highest population of the heteroclusters and the largest deviation from the ideal mixture appears at equimolar mixture.

2DCOS-NIR and chemometric study on microheterogeneity in binary mixtures of aliphatic and aromatic hydrocarbons has shown that even relatively weak interactions like π - π or differences in molecular shapes may give rise to deviation from the ideality [27]. The extent of these deviations is small for aromatic/aromatic or aliphatic/aliphatic mixtures and increases for aromatic/aliphatic mixtures. The shape of molecules has a significant effect on the extent of deviation from the ideal mixture. If both components of the mixture have similar shapes (linear or cyclic), the molecules with the same probability form the homo- and heteroclusters, otherwise, increases the tendency for formation of the homoclusters. Since the homoclusters of both components resemble those in neat liquids, one can conclude that deviation from the ideal mixture is due to presence of the heteroclusters. Interesting information provides 2D correlation moving-window spectrum. Figure 6.9 displays the composition-dependent moving-window spectrum of n-hexane/benzene mixture. It is of note that the spectral changes from the aromatic and aliphatic parts are clearly

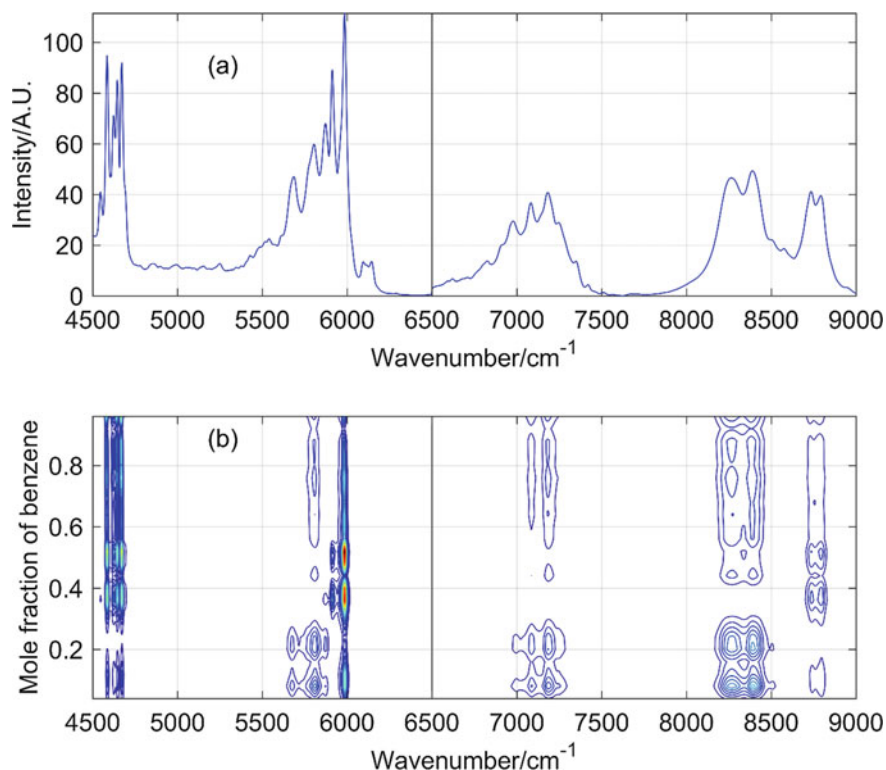
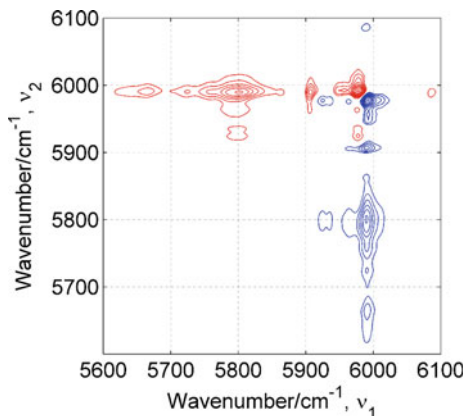


Fig. 6.9 A composition-average (a) and moving-window (b) spectrum for n-hexane/benzene mixture. Intensities in the 6500–9000 cm^{-1} range were enlarged to appear in this scale (Reprinted from Ref. [27] with permission from Elsevier)

separated. The maximum of spectral changes for n-hexane appears at mole fraction of benzene smaller than 0.3, while the largest changes for benzene are observed for mole fraction from 0.3 to 0.5. The differences observed in the moving-window spectra are nicely confirmed in the asynchronous spectra (Fig. 6.10). The spectrum develop the peaks between the overtones from the aliphatic and aromatic components of the mixture.

Shinzawa and Mizukado examined hydrogen/deuterium (H/D) exchange of gelatinized starch by using 2DCOS-NIR [28]. The time-dependent spectra reveal a series of subtle changes, which were resolved in the asynchronous contour plots. As shown, during the isotopic substitution, the exchange rate becomes different depending on solvent accessibility of various parts of the molecule. This way, it is possible to explore the local structure and dynamics of the sample. Zhou et al. have studied interactions in $\text{C}_2\text{H}_5\text{OH}/\text{CH}_3\text{CN}$ binary mixture by using NIR and MIR spectroscopy [29]. The data were converted to the excess absorption spectra and then analyzed by 2DCOS. The resolution enhancement in the excess and 2DCOS spectra permitted to identify a series of species including dimers, trimers and multimers of ethanol as

Fig. 6.10 Asynchronous 2D correlation spectrum constructed from NIR spectra of n-hexane/benzene mixture. In red and blue are drawn the positive and negative peaks, respectively



well as $C_2H_5OH-CH_3CN$ complex. As shown, the dissociation of ethanol multimers is correlated with an increase in the concentration of acetonitrile. At mole fraction of $X_{CH_3CN} = 0.7$, all multimers of ethanol are dissociated. Chang et al. applied 2DCOS-NIR to investigate combination bands of water perturbed by the presence of four different inorganic acids including: HCl , H_2SO_4 , H_3PO_4 and HNO_3 [30]. Analysis of the concentration-dependent 2DCOS contour plots evidenced that each of these acids has a different effect on NIR spectra of water.

Due to the resolution enhancement and selective correlation of various peaks, 2DCOS spectroscopy is a powerful tool for analysis of complex NIR spectra. The proper data pretreatment can substantially reduce the noise or baseline fluctuations and provide more reliable results. Sometimes, it is necessary to perform the normalization of the experimental data before application of 2D correlation analysis. Since publication of the principles of the generalized 2D correlation spectroscopy by Isao Noda in 1993, numerous modifications of this method were reported. These new developments extend the usefulness of the generalized 2DCOS and opens new possibilities of the spectral analysis. Among them, the most popular is the moving-window analysis, which provides the information on the dynamic changes in very simple and straightforward form. Similarly like chemometrics, 2DCOS prefers large data sets, especially for examination of complex processes. Nowadays, 2D correlation analysis is a routine tool for the spectral analysis, and its codes are included in the spectroscopic software.

References

1. I. Noda, Two-dimensional infrared (2D-IR) spectroscopy of synthetic and biopolymers. *Bull. Am. Phys. Soc.* **31**, 520 (1986)
2. I. Noda, Two-Dimensional Infrared (2D IR) spectroscopy: theory and applications. *Appl. Spectrosc.* **44**, 550–561 (1990)
3. I. Noda, Two-dimensional infrared spectroscopy. *J. Am. Chem. Soc.* **111**, 8116–8118 (1989)

4. I. Noda, Generalized two-dimensional correlation method applicable to infrared, raman, and other types of spectroscopy. *Appl. Spectrosc.* **47**, 1329–1336 (1993)
5. I. Noda, Y. Ozaki, *Two Dimensional Correlation Spectroscopy Applications in Vibrational and Optical Spectroscopy* (Chichester, UK, Wiley, 2004)
6. M.A. Czarnecki, Y. Morisawa, Y. Futami, Y. Ozaki, Advances in molecular structure and interaction studies using near-infrared spectroscopy. *Chem. Rev.* **115**, 9707–9744 (2015)
7. M.A. Czarnecki, Two-dimensional correlation analysis of hydrogen-bonded systems: basic molecules. *Appl. Spectrosc. Rev.* **46**, 67–103 (2011)
8. I. Noda, Determination of two-dimensional correlation spectra using the Hilbert transform. *Appl. Spectrosc.* **54**, 994–999 (2000)
9. M.A. Czarnecki, Two-dimensional correlation spectroscopy: effect of normalization of the dynamic spectra. *Appl. Spectrosc.* **53**, 1392–1397 (1999)
10. A. Gericke, S.J. Gadaleta, J.W. Brauner, R. Mendelsohn, Characterization of biological samples by two-dimensional infrared spectroscopy: simulation of frequency, bandwidth, and intensity changes. *Biospectroscopy* **2**, 341–351 (1996)
11. P.J. Tandler, P.B. Harrington, H. Richardson, Effects of static spectrum removal and noise on 2D-correlation spectra of kinetic data. *Anal. Chim. Acta* **368**, 45–57 (1998)
12. M.A. Czarnecki, Interpretation of two-dimensional correlation spectra: science or art? *Appl. Spectrosc.* **52**, 1583–1590 (1998)
13. M.A. Czarnecki, Two-dimensional correlation spectroscopy: effect of band position, width, and intensity changes on correlation intensities. *Appl. Spectrosc.* **54**, 986–993 (2000)
14. C. Zimba, *Presented at the Second International Symposium on Advanced Infrared Spectroscopy (AIRS II)* (Durham, NC, 1996)
15. S. Šašić, A. Muszynski, Y. Ozaki, A new possibility of the generalized two-dimensional correlation spectroscopy. 1. Sample—Sample Correlation Spectroscopy. *J. Phys. Chem. A* **104**, 6380 (2000)
16. S. Šašić, A. Muszynski, Y. Ozaki, A new possibility of the generalized two-dimensional correlation spectroscopy. 2. Sample—Sample and Wavenumber—Wavenumber Correlations of Temperature-Dependent Near-Infrared Spectra of Oleic Acid in the Pure Liquid State. *J. Phys. Chem. A* **104**, 6380–6387 (2000)
17. A. Watanabe, S. Morita, Y. Ozaki, Temperature-Dependent structural changes in hydrogen bonds in microcrystalline cellulose studied by infrared and near-infrared spectroscopy with perturbation-correlation moving-window two-dimensional correlation analysis. *Appl. Spectrosc.* **60**, 611–618 (2006)
18. M. Thomas, H.H. Richardson, Two-dimensional FT-IR correlation analysis of the phase transitions in a liquid crystal, 4'-n-octyl-4-cyanobiphenyl (8CB). *Vib. Spectrosc.* **24**, 137–146 (2000)
19. S. Morita, H. Shinzawa, R. Tsenkova, I. Noda, Y. Ozaki, Computational simulations and a practical application of moving-window two-dimensional correlation spectroscopy. *J. Mol. Struct.* **799**, 111–120 (2006)
20. S. Morita, H. Shinzawa, I. Noda, Y. Ozaki, Perturbation-correlation moving-window two-dimensional correlation spectroscopy. *Appl. Spectrosc.* **60**, 398–406 (2006)
21. I. Noda, Y. Liu, Y. Ozaki, M.A. Czarnecki, Two-dimensional Fourier transform near-infrared correlation spectroscopy studies of temperature-dependent spectral variations of oleyl alcohol. *J. Phys. Chem.* **99**, 3068–3073 (1995)
22. M. Kwaśniewicz, M.A. Czarnecki, MIR and NIR group spectra of n-alkanes and 1-chloroalkanes. *Spectrochim. Acta A* **143**, 165–171 (2015)
23. M. Kwaśniewicz, M.A. Czarnecki, The Effect of chain length on mid-infrared and near-infrared spectra of aliphatic 1-alcohols. *Appl. Spectrosc.* **72**, 288–296 (2018)
24. P. Tomza, M.A. Czarnecki, Microheterogeneity in binary mixtures of propyl alcohols with water: NIR spectroscopic, two-dimensional correlation and multivariate curve resolution study. *J. Mol. Liq.* **209**, 115–120 (2015)
25. W. Wrzeszcz, P. Tomza, M. Kwaśniewicz, S. Mazurek, R. Szostak, M.A. Czarnecki, Microheterogeneity in binary mixtures of methanol with aliphatic alcohols: ATR-IR/NIR spectroscopic, chemometrics and DFT studies. *RSC Adv.* **6**, 37195–37202 (2016)

26. W. Wrzeszcz, S. Mazurek, R. Szostak, P. Tomza, M.A. Czarnecki, Microheterogeneity in CH₃OH/CD₃OH mixture. *Spectrochim. Acta A* **188**, 349–354 (2018)
27. P. Tomza, W. Wrzeszcz, M.A. Czarnecki, Tracking small heterogeneity in binary mixtures of aliphatic and aromatic hydrocarbons: NIR spectroscopic, 2DCOS and MCR-ALS studies. *J. Mol. Liq.* **276**, 947–953 (2019)
28. H. Shinzawa, J. Mizukado, Hydrogen/deuterium (H/D) exchange of gelatinized starch studied by two-dimensional (2D) near-infrared (NIR) correlation spectroscopy. *Spectrochim. Acta A* **197**, 138–141 (2018)
29. Y. Zhou, Y. Zheng, H. Sun, G. Deng, Z. Yu, Hydrogen bonding interactions in ethanol and acetonitrile binary system: a near and mid-infrared spectroscopic study. *J. Mol. Struct.* **1069**, 251–257 (2014)
30. K. Chang, Y.M. Jung, H. Chung, Two-dimensional correlation analysis to study variation of near-infrared water absorption bands in the presence of inorganic acids. *J. Mol. Struct.* **1069**, 122 (2014)